

# Quantitative Spectroscopy of B-type Supergiants

D. Weißmayer<sup>1</sup>, N. Przybilla<sup>1</sup>, K. Butler<sup>2</sup>

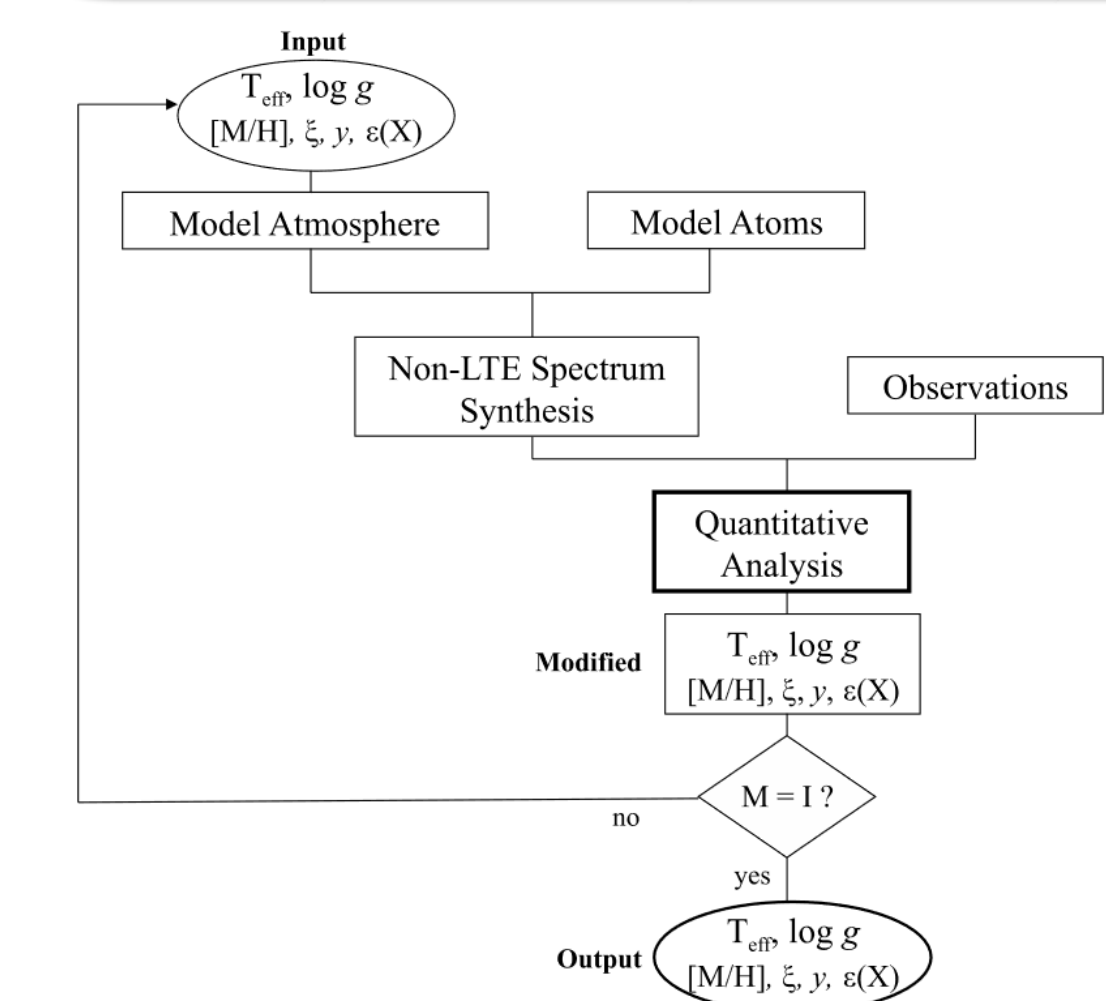
<sup>1</sup> Institut für Astro- und Teilchenphysik, Universität Innsbruck, Technikerstr. 25/8, 6020 Innsbruck, Austria

<sup>2</sup> LMU München, Universitätssternwarte, Scheinerstr. 1, 81679 München, Germany



## Introduction

B-type supergiants show enormous potential as resourceful tools to address a wide range of astrophysical questions concerning stellar atmospheres, stellar and galactic evolution, the characterisation of interstellar sightlines and the cosmic distance scale. For the purpose of a comprehensive analysis of these objects, we test a hybrid non-LTE approach – line-blanketed model atmospheres computed under the assumption of local thermodynamic equilibrium (LTE) in combination with line formation calculations that account for deviations from LTE – for a sample of 14 Galactic B-type supergiants with masses below  $30 M_{\odot}$ . The use of state-of-the-art model atoms of 12 chemical species allows us to determine the atmospheric abundances of all sample objects to an unprecedented degree. The analysed data is comprised of high signal-to-noise, high resolution spectra taken by the FEROS (La Silla, Chile) and FOCES (Calar Alto, Spain) spectrographs.



Ion	Terms	Transitions
H	20	190
He I	29+6	162
C II/III	68/70	425/373
N I/II	89/77	668/462
O I/II	51/176+2	243/2559
Ne I/II	153/78	952/992
Mg II	37	236
Al II/III	54+6/46+1	378/272
Si II/III/IV	52+3/68+4/33+2	357/572/242
S II/III	78/21	302/34
Ar II	56	596
Fe II/III/IV	265/60+46/65+70	2887/2446/2094

**Figure 1:** The parameters of the global solution for each individual object in the sample is given by an iterative procedure depicted in this flowchart [5].

**Table 1:** Model atoms used in the calculation of non-LTE level populations. The plus signs in the level column denote the number of superlevels.

## Models and Methods

For the calculation of synthetic stellar spectra, a hybrid non-LTE approach as outlined in Przybilla et al. (2006) [1] was used. In this approach plane-parallel model stellar atmospheres are calculated in LTE with the program Atlas12 [2], which serve as the basis for the calculation of the non-LTE level populations. The coupled radiative transfer and statistical equilibrium equations are solved with the program Detail [3]. Surface [4] then employs sophisticated line broadening theory and computes the final synthetic spectrum. For this procedure, we use state-of-the-art model atoms of 12 chemical species according to Table 1. The basic fitting process follows the flowchart of Figure 1. Grids of synthetic spectra are compared to all relevant spectroscopic indicators in an iterative fashion. A global solution is achieved, once all indicators are matched simultaneously.

## Testing the effects of turbulent pressure

The code Atlas12 takes the effects of turbulent motions with velocity  $v_{\text{turb}}$  (i.e., the microturbulent velocity) into account. A turbulent pressure term  $P_{\text{turb}} \propto v_{\text{turb}}^2$  is added in the model's hydrostatic equilibrium equation.

Comparing models with/without turbulent pressure showed:

- Turbulent pressure hardly changes the temperature, but noticeably lowers electron densities for  $\log \tau_R < 0$  (Fig. 2).
- In hydrogen lines, the increased pressure broadening leads to an increase of the derived surface gravity by  $\Delta \log g \approx 0.05$  dex. A shift in the ionisation balance affects lines of helium and metallic species (Fig. 3).

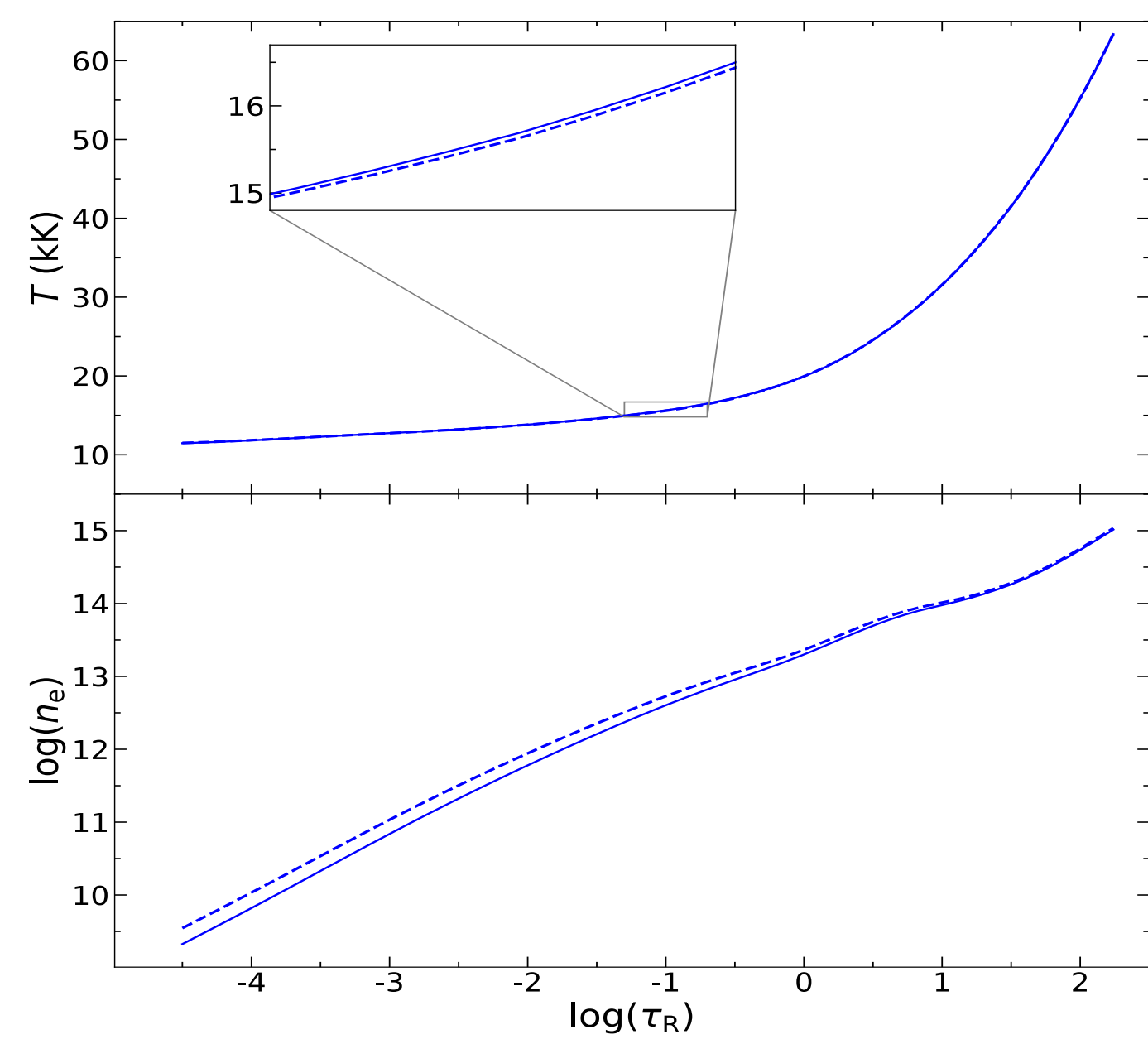


**Figure 2:** Temperature (upper panel) and electron density (lower panel) as a function of the logarithmic Rosseland optical depth. Displayed are Atlas12 stratifications computed with (full line) and without considering turbulent pressure (dashed line) for  $T_{\text{eff}} = 18\,600$  K,  $\log g = 2.45$  and microturbulence  $\xi = 14$  km s<sup>-1</sup>.

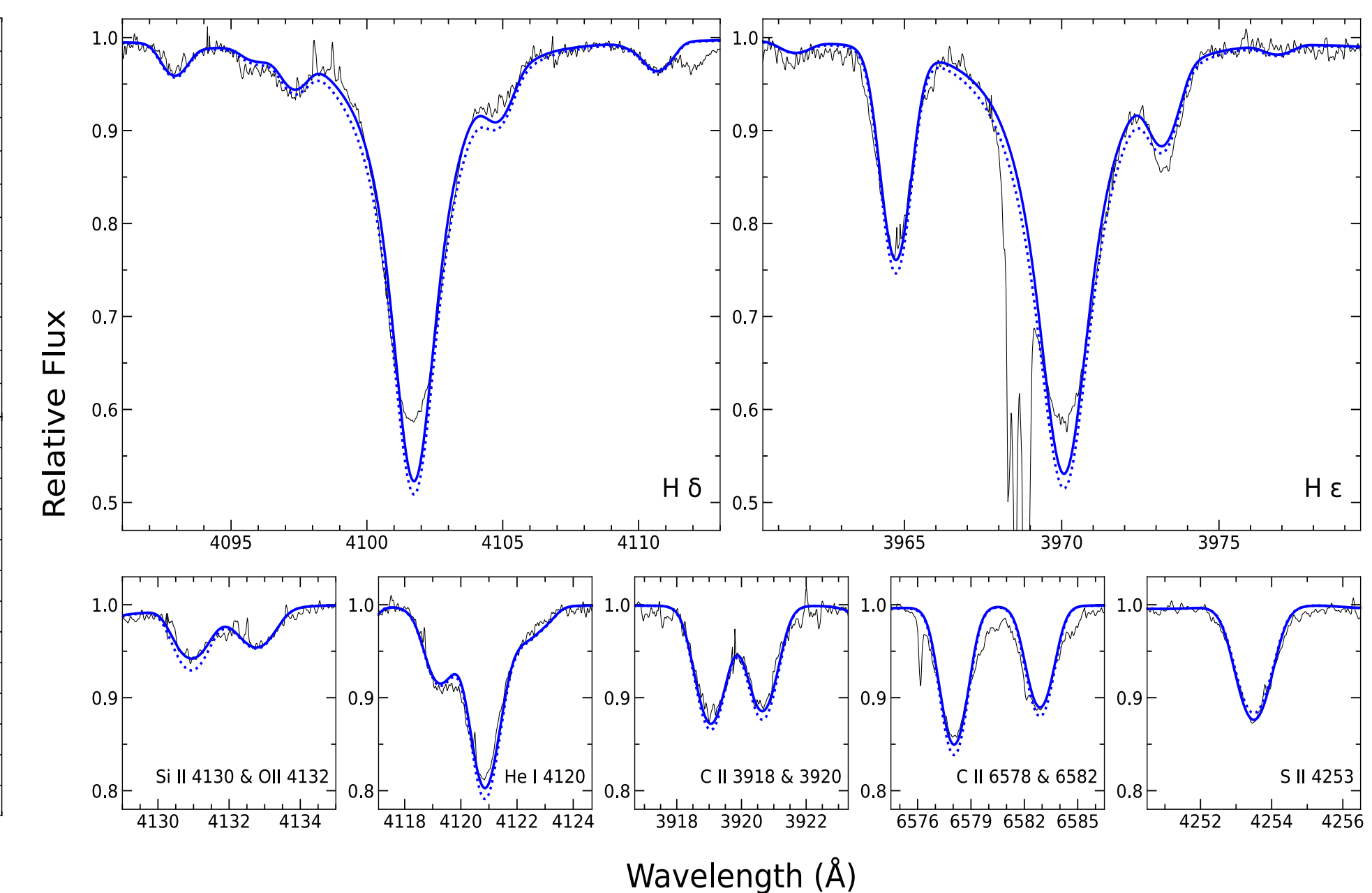


**Figure 3:** Effects of turbulent pressure on line profiles. The solid blue line depicts the best fitting synthetic spectrum for several diagnostic lines in the observed spectrum of HD 14818 (black) derived from model atmospheres that account for turbulent pressure. The dotted blue line depicts the same solution without assuming turbulent pressure.

## Results

- All spectroscopically accessible parameters ( $T_{\text{eff}}$ ,  $\log(g)$ ,  $v \sin(i)$ , micro- and macroturbulence and abundances) were successfully derived for the 14 sample objects.
- The global solution of each star tightly reproduces all observed spectral features simultaneously.
- The spectroscopic distances  $d_{\text{spec}}$  match the distances  $d_{\text{Gaia}}$  derived from Gaia EDR3 parallaxes [6], supporting the validity of the derived global solutions (Fig. 4).
- We derived mean abundances of helium and the 10 most abundant metal species; statistical uncertainties mostly range from  $\sim 0.05 - 0.1$  dex, and rarely exceed the latter value. The elemental abundances of C, N and O match the theoretical predictions of mixing by contemporary stellar evolution codes (Fig. 5).
- Consistency is achieved in star positions relative to evolution in the spectroscopic HRD and the HRD (Fig. 6).

## Comparison to previous analyses

- Overall good correlation of the effective temperatures  $T_{\text{eff}}^{\text{lit}}$  from the literature to those derived in this work (Fig. 7).
- Considerable scatter among different literature studies. A small, systematic shift towards higher  $\log g$  values in the present work may be noticed (Fig. 8)
- While our microturbulent velocities remain subsonic, literature values are often found to be supersonic (Fig. 9).

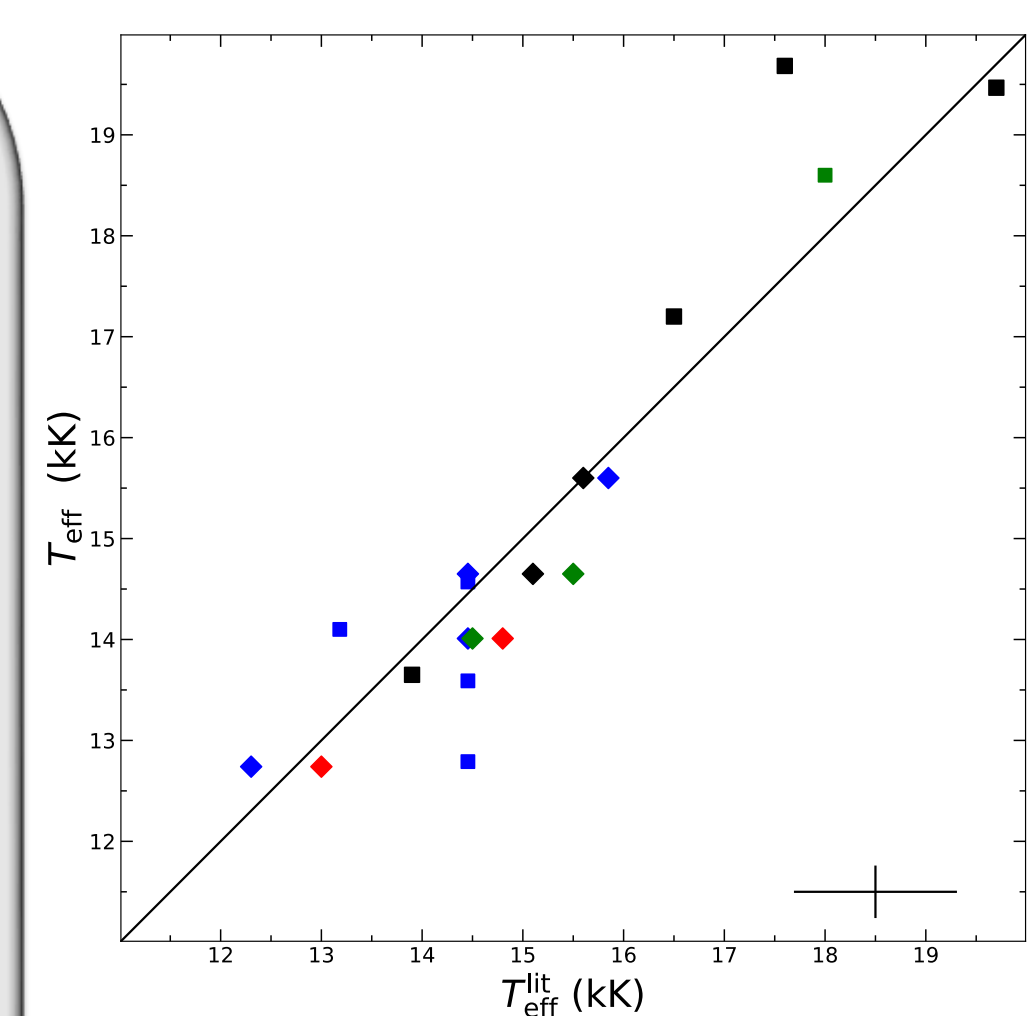


**Figure 7:** Comparison of deduced values of  $T_{\text{eff}}$  to parameters derived in previous work. Sample objects which appear in multiple compared studies are depicted as diamonds.

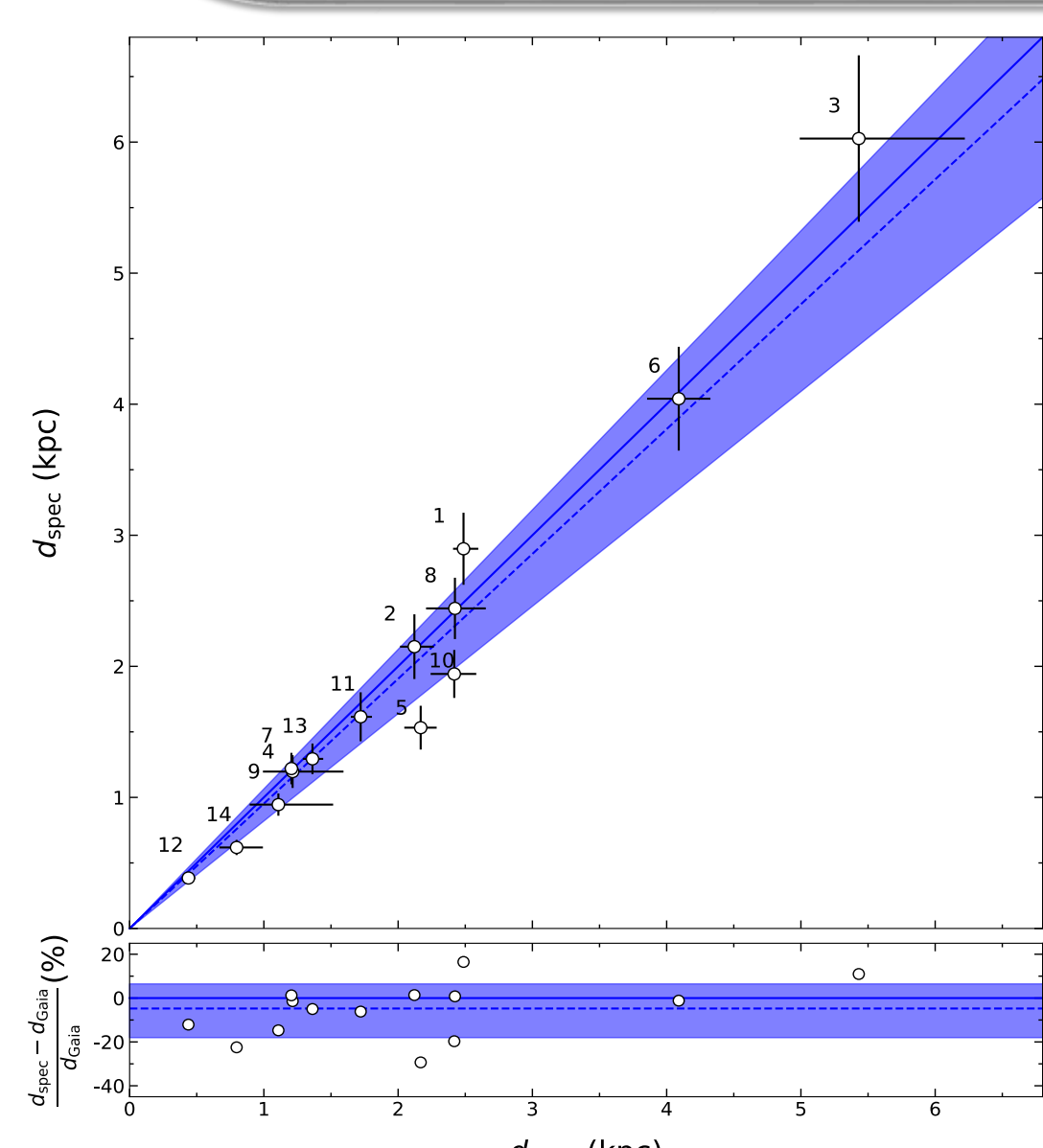


**Figure 4:** Correlation of spectroscopic distances  $d_{\text{spec}}$  and those derived from Gaia EDR3 parallaxes  $d_{\text{Gaia}}$ .

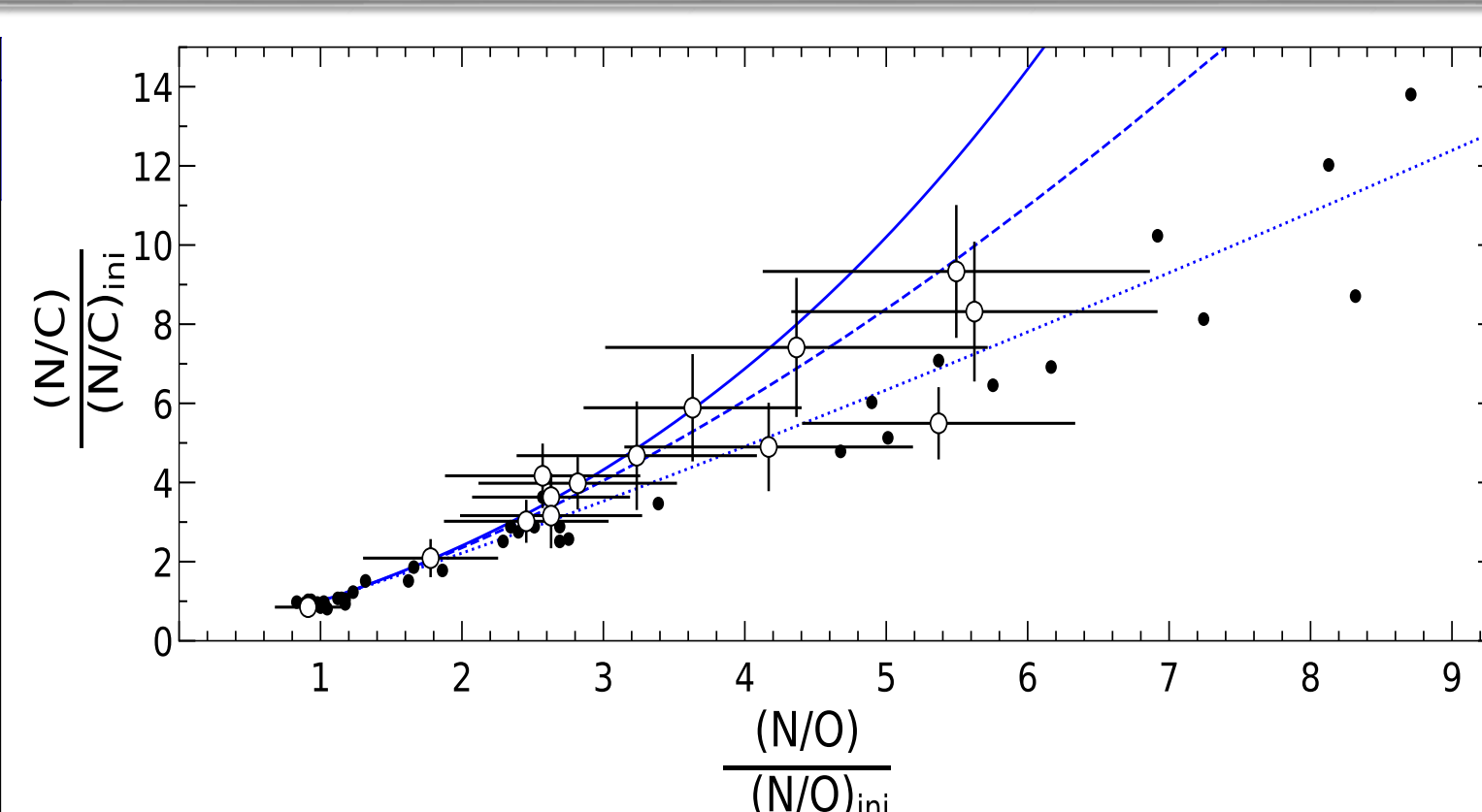


**Figure 5:** Location of the sample objects in the N/O-N/C plane tracing the effects of mixing. The values of the respective mass ratios (N/C and N/O) are normalized to the pristine abundances. Solid, dotted and dashed lines depict the theoretical nuclear paths of mixing in models of Georgy et al. (2013) [7] and Ekström et al. (2012) [8]. Values derived by Przybilla et al. (2010) [9] and observed values are depicted as black dots.

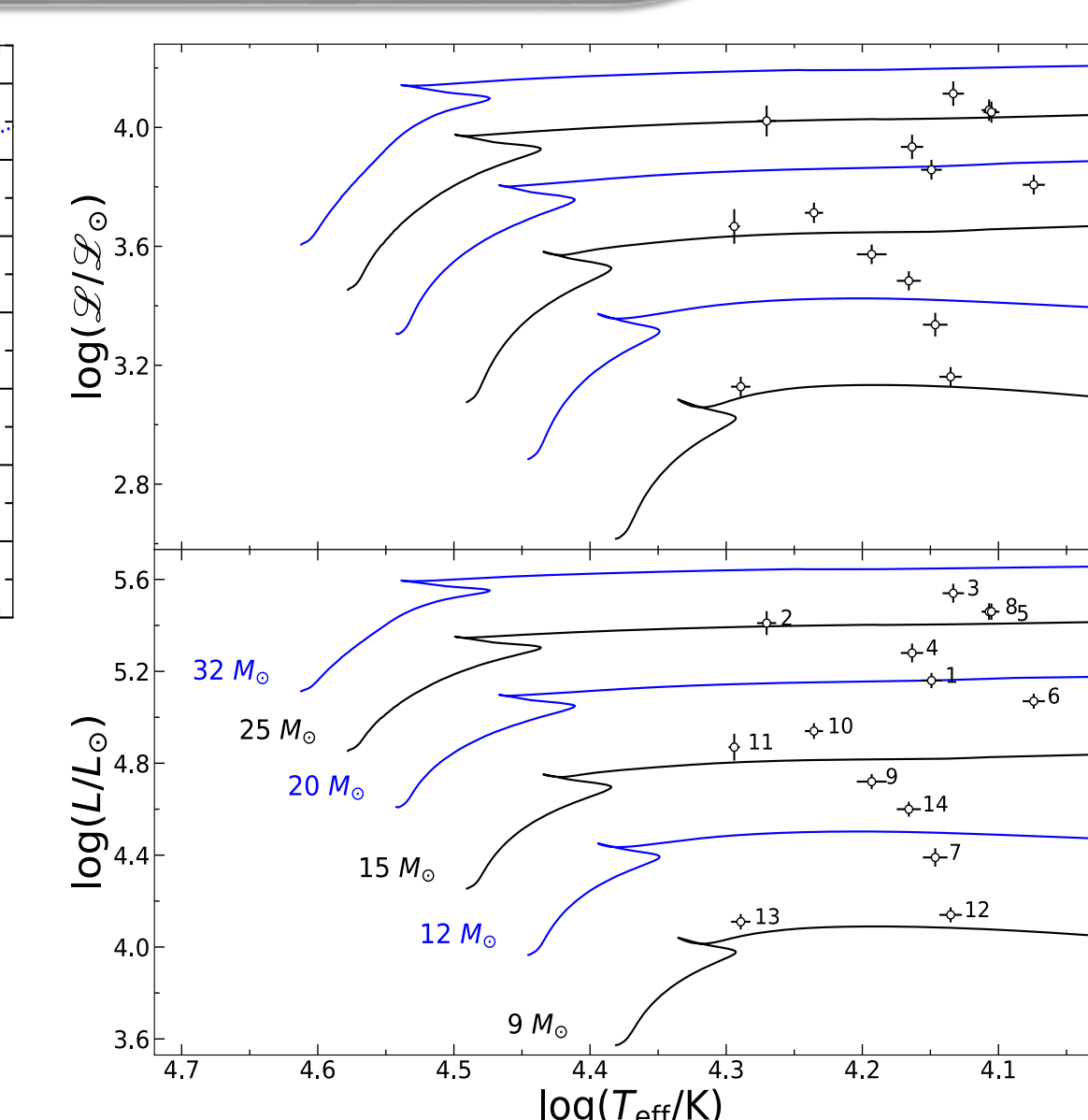


**Figure 6:** Stellar evolution models of various initial masses (Ekström et al. 2012)[8] and observed values of stellar luminosity and  $T_{\text{eff}}$  for the sample objects.

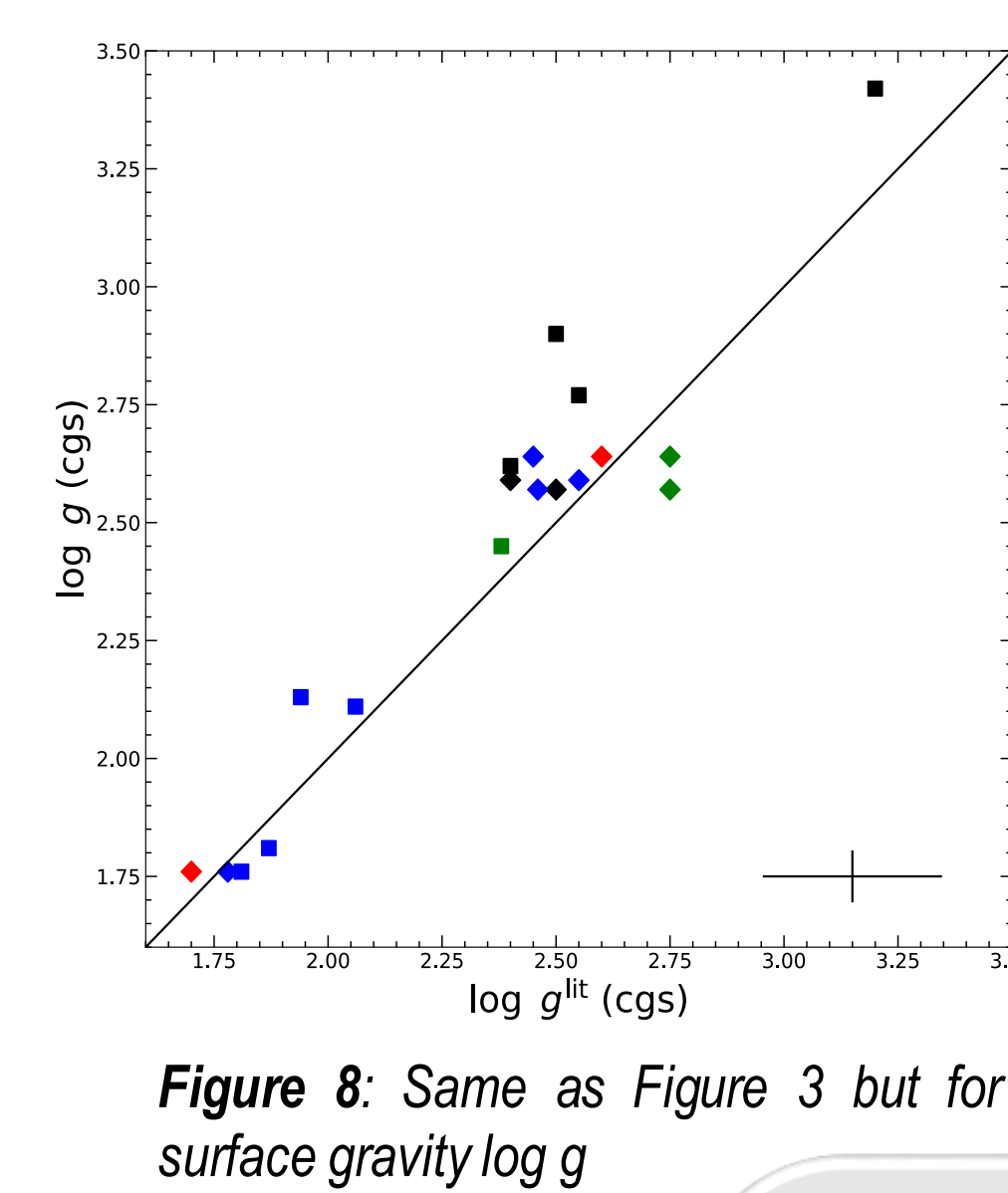


**Figure 8:** Same as Figure 3 but for surface gravity  $\log g$

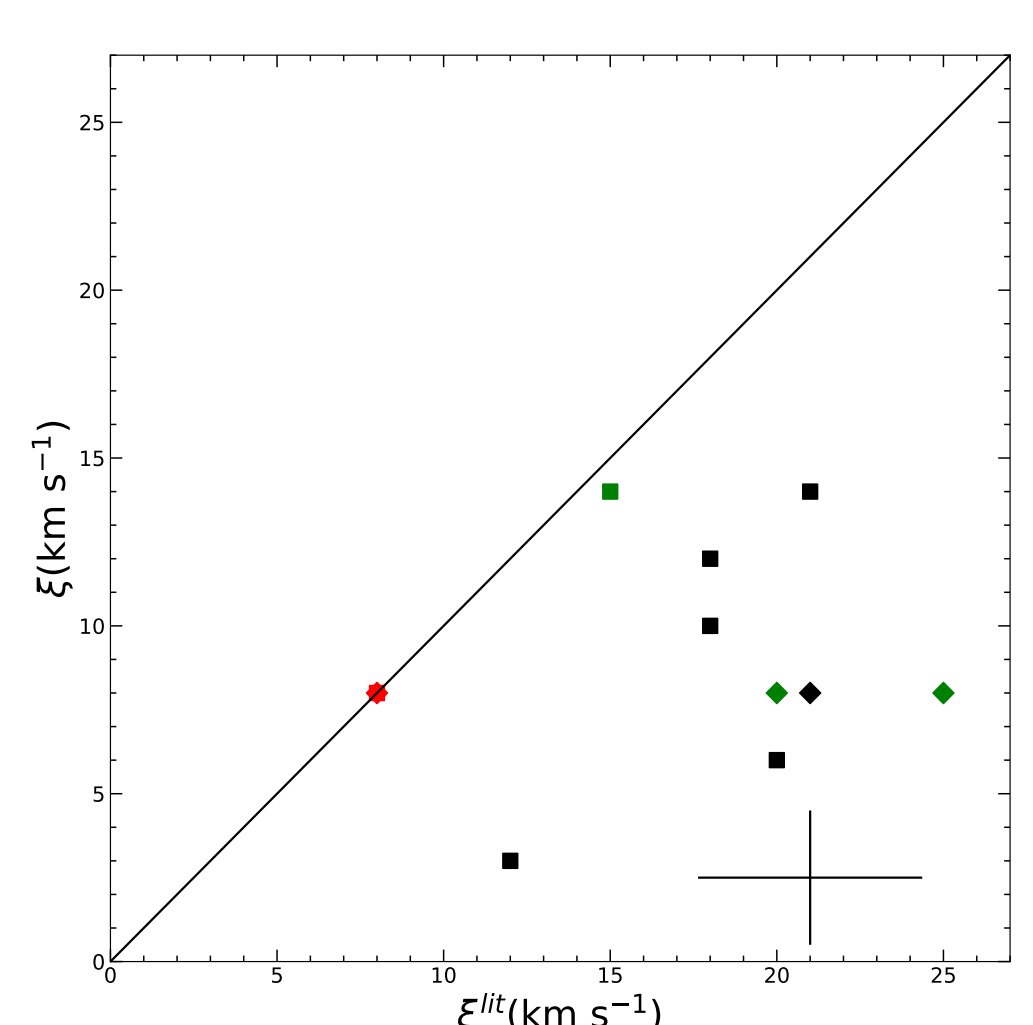


**Figure 9:** Same as Figure 3 but for microturbulence  $\xi$

## Conclusions

The described methodology was used in a comprehensive analysis of a set of 14 B-type supergiants, the solutions for which tightly reproduce the observed spectra. The derived parameters were set into context with contemporary models of stellar evolution, directly compared to previous analyses and scrutinized by various tests for consistency. Significantly, turbulent pressure, as accounted for by Atlas12, was shown to become relevant for microturbulent velocities larger than 10 km s<sup>-1</sup>.

## References:

- [1] Przybilla, N., Butler, K., Becker, S. R., & Kudritzki, R. P. 2006, A&A, 445, 1099
- [2] Kurucz, R. L. 2005, Mem. Soc. Astron. Ital. Suppl., 8, 14
- [3] Giddings, J. R. 1981, PhD thesis (Univ. London)
- [4] Butler, K. & Giddings, J. R. 1985, Newsletter of Analysis of Astronomical Spectra, 9 (Univ. London)
- [5] Nieva, M.-F. & Przybilla, N. 2012, A&A, 539, A143
- [6] Gaia Collaboration, Brown, A. G. A., Vallenari, A., et al. 2021, A&A, 649, A1
- [7] Georgy, C., et al. 2013, A&A 553, A24
- [8] Ekström, S., Georgy, C., Eggenberger, P., et al. 2012, A&A, 537, A146
- [9] Przybilla, N., et al., 2010, A&A 517, A38